SMALL GTPASES
2021, VOL. 12, NO. 4, 265–272
https://doi.org/10.1080/21541248.2020.1826781

Taylor & Francis
Taylor & Francis Group

BRIEF REPORT

Exploring a role for fatty acid synthase in prostate cancer cell migration

Mario De Piano[a], Valeria Manuelli[a], Giorgia Zadra[b], Massimo Loda[b], Gordon Muir[c], Ash Chandra[d], Jonathan Morris[a], Mieke Van Hemelrijck [a], and Claire M. Wells[a]

[a]School of Cancer and Pharmaceutical Sciences, Kings College London, London, UK; [b]Departments of Oncologic Pathology and Pathology, Dana-Farber Cancer Institute and Brigham and Women's Hospital, Harvard Medical School, Boston, USA; [c]Urology, King's College Hospital, London, UK; [d]Cellular Pathology, St. Thomas' Hospital, London, UK

ABSTRACT

Fatty acid synthase (FASN) is commonly overexpressed in prostate cancer and associated with tumour progression. FASN is responsible for *de novo* synthesis of the fatty acid palmitate; the building block for protein palmitoylation. A functional role for FASN in regulating cell proliferation is widely accepted. We recently reported that FASN activity can also mediate prostate cancer HGF-mediated cell motility. Moreover, we found that modulation of FASN expression specifically impacts on the palmitoylation of RhoU. Findings we will describe here. We now report that loss of FASN expression also impairs HGF-mediated cell dissociation responses. Taken together our results provide compelling evidence that FASN activity directly promotes cell migration and supports FASN as a potential therapeutic target in metastatic prostate cancer.

ARTICLE HISTORY
Received 17 July 2020
Revised 14 September 2020
Accepted 17 September 2020

KEYWORDS
Fatty acid synthase; prostate cancer; RhoU

Brief report

Prostate cancer is the most commonly diagnosed non-cutaneous malignancy in the world and is leading cause of cancer-related deaths in the western population [1]. The five-year survival rate of patients drops to 28% if the prostate cancer has spread to other parts of the body [2]. Moreover, despite increased effort in the area of early detection, 10–20% of cases still present with widespread metastasis at the time of diagnosis [3]. Thus, there is an urgent need to better understand progressive disease to facilitate the development of novel biomarkers of aggressiveness and deliver novel therapeutics to target disseminating cells.

A prerequisite of metastasis is the adoption of a migratory phenotype by cancer cells [4] as they navigate the stroma, enter vasculature and spread to distant organs or tissues [4]. Such migration relies on the continuous reorganization of the actin cytoskeleton, which can be triggered by a variety of extracellular stimuli via the activity of Rho family GTPases; the master regulators of the actin cytoskeleton [5]. Rho GTPase proteins are frequently post-translationally modified by lipids via palmitoylation and/or prenylation, which promotes specific subcellular localization to membrane compartments that directly influence downstream signalling [5]. In addition to changes in motile properties it has long been recognized that cancer cells exhibit alterations in their metabolic activity compared to untransformed cells. This metabolic reprogramming increases the production of metabolic intermediates required to support rapid proliferation [6]. Part of the change in metabolic activity is the initiation of *de novo* fatty acid (FA) synthesis. Indeed, increased lipogenesis is recognized as a major hallmark for tumour progression, with cancer cells switching to dependence on *de novo* fatty acid (FA) synthesis [6]. The main metabolic enzyme responsible for the generation of FA in the cell is Fatty Acid Synthase (FASN) [7] which is consistently overexpressed in prostatic tumours [8,9]. A considerable amount of research has focused on how FASN activity can promote cellular proliferation [7] but little attention has been paid to other potential cellular consequences of increased FASN expression in the cancer setting. Interestingly, there was some evidence in the literature to suggest FASN could directly influence cell migration, indeed reduced expression of FASN has been associated with impaired cell migration in prostate, osteosarcoma and colorectal cancer cells [10,11,12]. Importantly metastasis initiating cells upregulate their FA availability via the CD36 receptor [13] and this event is required to drive distal site colonization. However, the molecular mechanisms through which increased levels of intracellular FA drive metastasis have yet to be elucidated. Thus, we were interested to specifically

CONTACT Claire M. Wells claire.wells@kcl.ac.uk School of Cancer and Pharmaceutical Sciences, Kings College, London

explore in more detail whether FASN activity was an important component of cell migration.

Our studies confirmed that FASN is expressed at detectable levels in cancer cells lines that are known to exhibit mesenchymal modes of migration [14–16] (Figure 1a,b) but is also expressed at comparable levels in cell lines that are more epithelial in nature [17]. Moreover, we detected expression in PC3 and 1542-CPTX (subsequently referred to as 1542 cells) prostate cancer cell lines (Figure 1a,b); 1542 cells were derived from a radical prostatectomy via SV40 transformation and represent cells within the primary tumour with potential migratory capacity [18]. We further expanded this study to consider whether we could detect high levels of FASN protein in human prostate cancer tissue taken from tumour samples collected by radical surgery. These tumour samples were graded by a pathologist (Figure 1c) with respect to the extent of malignant tissue present. Interestingly, we found high FASN expression in all tumour tissues independent of tumour amount (Figure 1d). Moreover, compared to the highest level of FASN expression in normal tissue (H5) all the samples with malignant cells exhibited a statistically significant increase in FASN protein level (Figure 1e). Encouraged by this evidence that FASN functionality might extend beyond just promoting proliferation we sought to investigate cell migration. Moreover, we planned to question if the contribution of FASN functionality was via generation of palmitate or an alternative pathway.

Initially to explore the relationship between FASN and cell migration we reduced FASN expression in 1542 and PC3 cells using ShRNA technology. We confirmed that these cells do indeed display a proliferation defect [19] and thus we chose our migration assays carefully to avoid overlapping phenotypes. To explore any perturbation of cell migration in FASN depleted cells we made time-lapse movies of control and FASN depleted cells and measured cell migration speeds. We detected a significant reduction in HGF-stimulated mean cell migration in all the FASN shRNA treated cell lines compared to control [19]. Indeed, the reduction in cell migration speed was not matrix dependent; as we can now demonstrate the same reduction in cell speed on a collagen substrate (Figure 2) using the same cells as described in [19]. Furthermore, in a HGF-independent-inverted invasion assay FASN shRNA cells were again unable to invade the collagen matrix when compared with control cells [19]. Moreover, the same inhibition of migration could be delivered using specific inhibitors of FASN lipogenic activity [19]. The inhibition of migration by the FASN inhibitors confirms the importance of lipogenic activity and points to a requirement in these cells for endogenously produced palmitate. These results were delivered in a HGF-stimulated random migration assay. We have now tested a second prostate cancer cell migration model. Here we are using HGF to stimulate cell: cell dissociation and adoption of a cell migration phenotype in DU145 prostate cancer cells [17]. Importantly, we find that a 70% FASN depletion (Figure 3a) also significantly reduces HGF-induced cell scattering of these cells (Figure 3b,c). Having established that cells with reduced expression of FASN exhibited impaired motility we sought to understand the mechanism linking loss of FASN (and specifically loss of FASN activity) to cell migration defects. We know from previous studies that impaired migration is often the result of changes in the dynamics of the actin cytoskeleton and/or changes in the way that cells interact with the underlying matrix. Interestingly, we detected changes in both cell matrix adhesion and cell shape in our FASN depleted cells [19].

First, detailed observation of matrix adhesion revealed that FASN depleted cells exhibited prominent paxillin associated peripheral cellular adhesions [19]. Importantly, addition of exogenous palmitate rescued the adhesion phenotype whilst having no impact on FASN expressing cells demonstrating the dependence of cells on palmitate to manage optimal matrix adhesion. A preponderance of peripheral adhesions can either point to enhanced adhesion formation or a reduction in the rate of adhesion turnover. Our previous work has highlighted an important role for RhoU in regulating adhesion turnover [15] where targeted deletion of RhoU leads to prominent paxillin associated peripheral cellular adhesions. RhoU was directly linked to adhesion turnover via regulation of paxillin phosphorylation at serine 272 (S272) [15]. Interestingly, we found that paxillin S272 phosphorylation was reduced in our FASN depleted cells [19]. It has been suggested that RhoU might be palmitoylated [20] and we thought that perhaps RhoU could be sensitive to a reduction in available palmitate in FASN depleted cells and this might prevent its activity towards paxillin mediated regulation of adhesion turnover. Using a standard palmitoylation assay we were able to demonstrate that RhoU is indeed palmitoylated and further show that RhoU palmitoylation was reduced in a background of FASN depletion. Moreover, palmitoylation of RhoU was required to support adhesion turnover [19]. Thus, the reduced cell migration speed of FASN depleted prostate cancer cells is in part attributed to increased matrix adhesion.

Not only did we detect a change in cellular adhesion we also noted that FASN depleted cells exhibited on average a smaller cell spread area. This phenotype is also replicated in our newer studies of DU145 cells

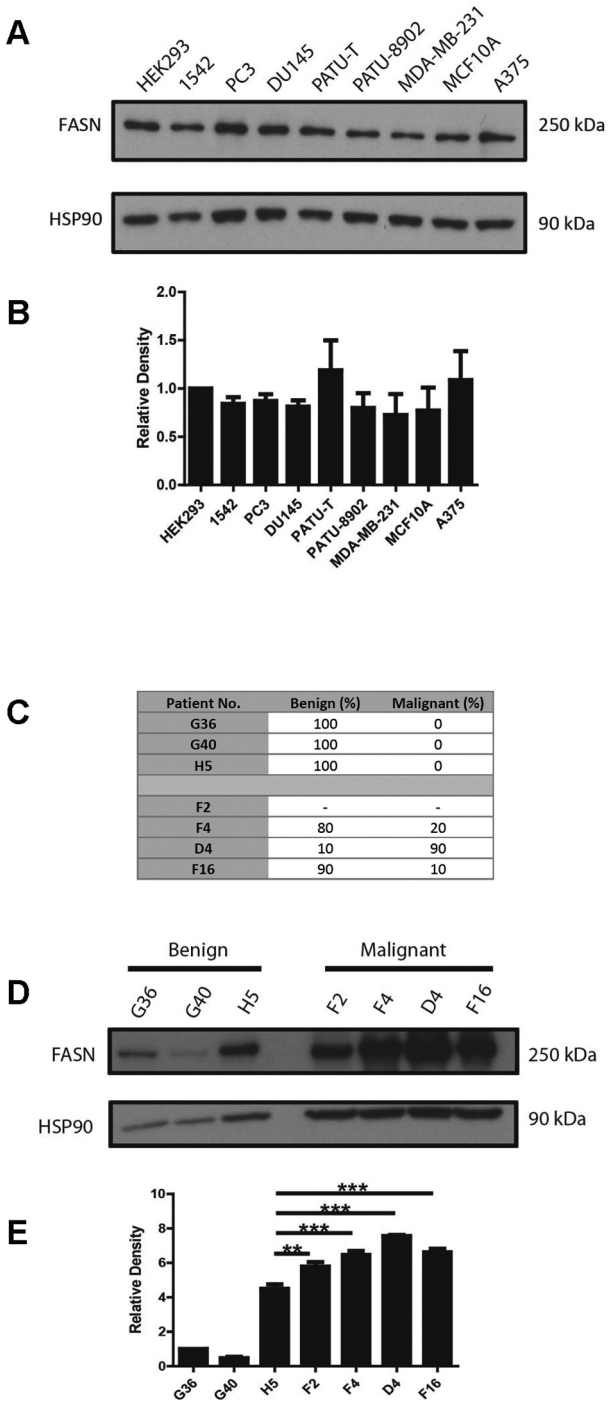

Figure 1. FASN is expressed in migratory cells and malignant tissue.

(a) Whole cell lysates were prepared from a range of cancer cell lines as illustrated. These were then subjected to SDS-PAGE and immunoblotted for FASN and the loading control HSP90. (b) Densitometry analysis was performed and relative quantification of FASN levels calculated. (c) Human primary prostate tissue was excised by surgical biopsy from seven different patients. Histopathological analysis of stained sections was performed and the approximate % of benign and malignant material was documented. Tumour percentage unknown for F2; but malignant diagnosis was confirmed for this sample. (d) proteins were extracted from the tissue samples and probed for FASN expression levels via SDS-PAGE gel electrophoresis HSP90 was used as a loading control. (e) Densitometry analysis was performed and relative quantification of FASN levels calculated. Data represents the mean values ± SEM from three independent experiments. Statistical significance was determined by student's one-way ANOVA with Tukey's post-hoc test. ** $p < 0.01$, ***$p < 0.001$.

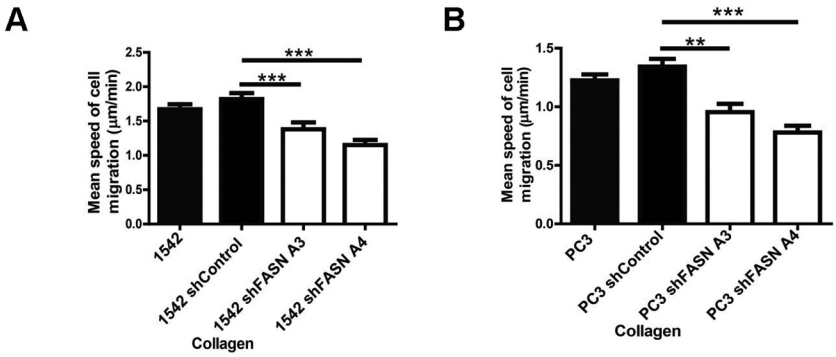

Figure 2. FASN depleted cells exhibit reduced migration speed on collagen.

(a) 1542, 1542 shControl, 1542 shFASN A3 and 1542 shFASN A4 cells were seeded into collagen coated wells, serum starved, stimulated with 10 ng/ml HGF and imaged for 16 h with images being taken at 5 minute intervals. Migration plots of each cell line trajectory were created (60 cells per condition). Cell tracking data was placed into a Mathematica notebook and then the speed of cell migration was calculated as described in methods. (b) PC3, PC3 shControl, PC3 shFASN A3 and PC3 shFASN A4 cells were seeded into matrigel coated wells and treated as above (a).

(Figure 3d). RhoU has not been linked to cell spread area but another Rho family GTPase Cdc42, that can also be modulated by palmitoylation, has been associated with the regulation of cell spread area [21]. Further exploration led us to discover that depletion of FASN induces a loss of total Cdc42 expression. We were surprised to discover that the Cdc42 isoform expressed in our cells is not the palmitoylated variant [22] and that the reduction we detected was in expression of canonical Cdc42 [19]. We next sought to understand why Cdc42 protein levels were reduced in FASN depleted cells. We hypothesized that perhaps there was a relationship between RhoU and Cdc42 that was palmitate dependent. Interestingly, we were able to demonstrate that Cdc42 protein levels are very sensitive to modest reductions in RhoU expression. Moreover, using a global inhibitor of palmitoyltransferase activity we confirmed that canonical Cdc42 protein levels are dependent on protein palmitoylation. Finally, we could demonstrate that RhoU and Cdc42 co-immunoprecipitate from cells [19]. Having evidenced in vitro that changes in FASN expression could influence cell migratory behaviour we looked to translate our findings to the clinical setting. Using data held in The Cancer Genome Atlas (TCGA) we found that there is a highly significant difference in RhoU expression and a trend towards significant difference in Cdc42 expression when comparing mRNA signals in low and high Gleason score samples. Moreover, we stained benign tissue, Dominant Gleason (DG) and Highest Gleason (HG) grade prostate tissue samples and found that both DG and HG were significantly associated with an increase in the expression of FASN, RhoU, and Cdc42 [19] compared to benign tissue.

Taken together our results have lead us to hypothesize that in a cancer cell with an increased level of FASN expression there is both a proliferative and invasive advantage. We propose that the invasive advantage correlates with the increased availability of de novo synthesized palmitate (Figure 4). Amongst the proteome of potential palmitoylated proteins, we find evidence that palmitate levels directly influence RhoU mediated cell adhesion turnover and promote canonical Cdc42 stabilization. We speculate that in these prostate cancer cells FASN synthesizes palmitate which is used in the palmitoylation of RhoU via DHHC PATs [23]. Palmitoylated RhoU binds prenylated Cdc42 and both proteins tether to the cell membrane where Cdc42 can be activated [5]. Here, Cdc42 and RhoU signal and activate downstream effector proteins which induce changes in the actin cytoskeleton that mediate cellular morphology. RhoU is also involved in mediating the turnover of focal adhesions through driving paxillin phosphorylation. These signalling events allow for unperturbed cell spreading and migration. In a FASN knockdown or inhibited cell, palmitate synthesis is severely diminished, significantly reducing RhoU palmitoylation, leading to its cytosolic accumulation. Palmitoylated RhoU is no longer able to sequester Cdc42 away from the ubiquitin ligases [24] which lead to it being targeted for degradation. Moreover, the prevention of RhoU palmitoylation leads to a decrease in paxillin phosphorylation which impedes focal

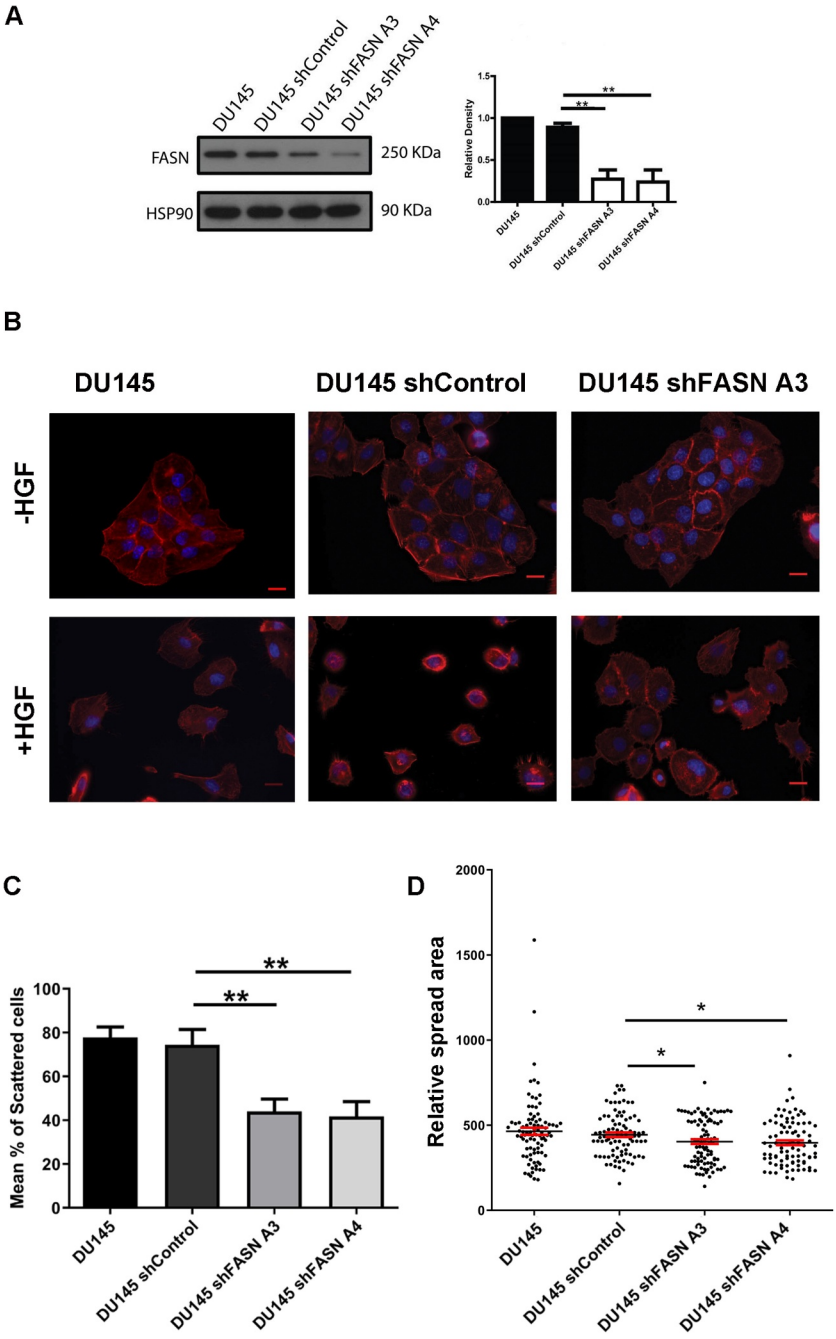

Figure 3. HGF-induced cell scattering is diminished in FASN depleted cells.

(a) Whole cell lysates were prepared from DU145, DU145 shControl, DU145 shFASN A3 and DU145 shFASN A4. These were then subjected to SDS-PAGE and immunoblotted for FASN and the loading control HSP90. Densitometry analysis was performed and relative quantification of FASN levels calculated. (b) DU145, DU145 shControl, DU145 shFASN A3 cells colonies were seeded on coverslips, serum starved for 24 hours, then incubated with or without HGF (10 ng/ml) for 24 hours. Cells were fixed and stained for F-actin (red) and DAPI (blue). (c) For each population indicated 90 cells were counted over 3 independent experiments and scored for single cell (scattered) or within a colony. mean ± S.E.M. Statistical significance was determined by a student's Anova *Tukey test. n.s.d = No statistical difference* ** $p < 0.005$ (d) DU145, DU145 shControl, DU145 shFASN A3 and DU145 shFASN A4 cells were seeded on matrigel and incubated for 24 hours. Cells were fixed and stained for F-actin and DAPI. Images were quantified for cell spread area 90 cells per condition over 3 independent experiments see methods for details. mean ± S.E.M. Statistical significance was determined by a student's Anova *Tukey test. n.s.d = No statistical difference* * $p < 0.05$

adhesion turnover. Thus, perturbed RhoU and Cdc42 signalling as a result of targeting FASN activity reduces cell spreading and migration. In conjunction with the tissue expression analysis these studies strongly support blocking the activity of FASN in prostate cancer cells as an attractive therapeutic pathway in advanced disease.

Materials and methods

Antibodies

Mouse anti-FASN were obtained from BD Biosciences and rabbit anti- HSP90 from Santa-Cruz Biotechnology. HRP-conjugated secondary antibodies were purchased from DAKO.

Cell culture

DU145 and PC3 prostate cancer cells were obtained from the European Tissue Culture Collection and grown in RPMI 10% FBS (Sigma-Aldrich) and 100 U/ml penicillin/streptomycin. The 1542-CPTX [18] primary prostate cancer cell line (herein referred to as 1542 cells), kindly gifted by Prof. John Masters (UCL), was grown in KSFM supplemented with 10% FBS, 0.1 mg/ml bovine pituitary extract, 5 ng/ml EGF and 100 U/ml penicillin/streptomycin. HEK-293 cells, MDA-MB-231, PaTU-8902, and PaTU-8988 T cells (European Tissue Culture Collection) were grown in complete DMEM (Sigma-Aldrich) supplemented with 10% FCS (Sigma-Aldrich) and 100 U/ml penicillin/streptomycin. MCF-10A were obtained from the European Tissue Culture Collection and grown in DMEM/F12 supplemented with 10% FBS (Sigma-Aldrich) 100 U/ml penicillin/streptomycin, EGF (100 mg/ml), Hydrocortizone (1 mg/ml): Cholera Toxin (1 mg/ml) and Insulin (10 mg/ml). A375 melanoma cells were obtained from the European Tissue Culture Collection and grown in DMEM/F12 10% FBS (Sigma-Aldrich) and 100 U/ml penicillin/streptomycin.

Tissue preparation for western blotting

Prostate tissue samples were taken from patients [Ethics REC 08/H0804/114] who underwent prostate surgery at Kings College London Hospital, Denmark Hill, London. Three of the samples are from patients with benign prostatic hyperplasia (G36, G40 and H5) and four of the samples are from patients with prostate cancer (F2, F4, D4 and F16). Prostate samples were extracted using RIPA buffer (20 nM Tris-HCl pH7.4, 150 mM NaCl, 1 mM EDTA, 1% Triton X-100, 0.5% SDS, and 1% sodium dexycholate) and incubated on ice for 20 minutes. Samples were homogenized with scalpel tearing and vortexing prior to high pulse centrifuging for 3 minutes at 4°C followed by additional homogenization with a needle. The liquid sample was recovered and the appropriate volume of 6 x gel sample buffer added based on Bradford protein quantification. Samples were then heated at 95°C for 5 minutes and stored at −80°C.

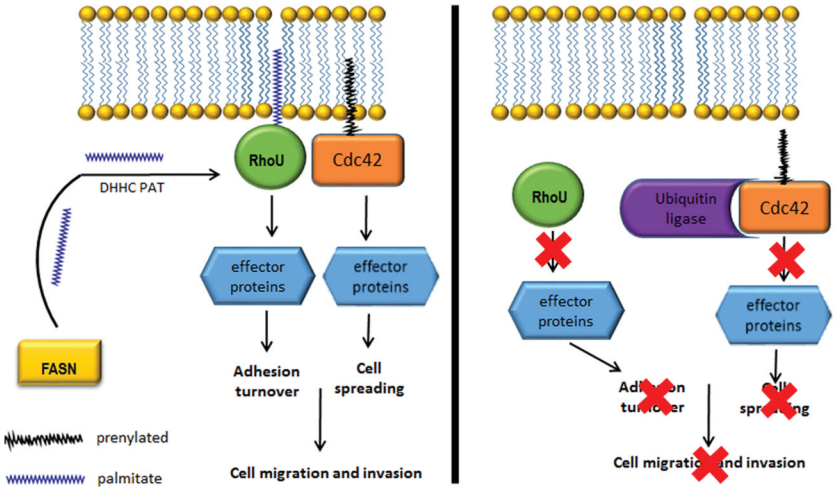

Figure 4. FASN activity supports RhoU and Cdc42 regulation of cell migration.
Proposed model of the impact of loss of FASN activity (and therefore palmitate production) on prostate cancer cell migration and invasion.

shRNA transfection

For stable knockdown of FASN in DU145, PC3 and 1542 cells 293 T cells were transfected with lentiviral constructs(PLKO.1) together with packing plasmids Delta 8.9 and VSV-g using Fugene HD (Promega). Lentiviral constructs containing two different shRNA sequences generated by the RNAi Consortium (Broad Institute Cambridge) shFASN A3(CATGGAGCGTATCTGTGAGAA),shFASNA4 (CGAGAGCACCTTTGATGACAT), shControl (ACAACAGCCACAACGTCTATA). Supernatant containing lentivirus was used to infect target cells in the presence of 5ug/ml polybrene. Cells were selected with 2ug/ml puromycin (Sigma).

Migration assay

Cells were plated onto collagen-coated 6-well plates to which 20 mM Hepes was added. Immediately prior to filming, cells were treated with 20 ng/ml HGF [14]. Each plate was placed on the automated heated stage of an Olympus IX71 microscope set at 37°C and imaged with a 10X/NA 0.3 UPlanFLN objective lens. Images were collected using a Retiga SRV CCD camera, taking a frame every 5 min for up to 16 h using Image-Pro Plus software. Subsequently, all the acquired time-lapse sequences were displayed as a movie and cells were tracked for the whole of the time-lapse sequence using ImageJ [25]. At least 60 cells were tracked over 3 separate films for each experimental condition. Mathematical analysis was then carried out using Mathematica 6.0™ notebooks developed in house [25]. Statistical significance was accepted for $p \leq 0.05$.

HGF-induced scatter assay

Cells were seeded onto coverslips at a cell density of 1.5 × 104/ml and incubated for 24 h. Cells were then serum starved with RPMI 160 + 0.5% FBS media for 24 h HGF (10 ng/ml) was added to the media and then plates were left for a further 24 h. Cells were then fixed in 4% paraformaldehyde after 24 h and stained for F-actin and DAPI. Images were taken of multiple fields of view. Cells were counted and cell counts of minus HGF were compared to plus HGF. The % of scattered cells per experiment was calculated by scoring the number of scattered (cell has junction with one or more other cells) and scattered (no cell: cell contacts) cells per field of view.

Immunoblotting

Cells were lysed for 10 min in lysis buffer (0.5% NP-40, 50 mM Tris-HCl pH 7.5, 150 mM NaCl, 5 mM EDTA, 50 mM NaF, 1 mM Na3VO4, 1 mM PMSF, 10 µg/ml leupeptin and 1 µg/ml aprotinin) and clarified by centrifugation at 13,000 x g for 10 min. Proteins were resolved by SDS-PAGE as previously described [26] and immunoblotted with the relevant antibodies. Proteins were detected using an ECL detection kit (Pierce) and autoradiographs were scanned for densitometry analysis.

Immunofluorescence and image analysis

Cells were fixed in 4% paraformaldehyde for 20 min at RT and subsequently permeabilised with 0.2% Triton X-100 for 5 min. Cells were incubated with TRITC-conjugated phalloidin (Invitrogen) and DAPI (Sigma) diluted in PBS for 1 h at RT. Following incubation, cells were washed 3 times in PBS. Stained cells were imaged using an Olympus IX71 microscope with a 40X/NA 1.3 UPlanFLN oil-immersion objective and Image-Pro Plus software (supplied by MAG, UK). ImageJ software was used to calculate cell spread area based on F-actin staining.

Statistics

The Anova *post hoc Tukey test* was used in all analysis and values were considered statistically significant if $p = \leq 0.05^{*}$, $p = \leq 0.005^{**}$, $p = \leq 0.005^{***}$.

Disclosure statement

No potential conflict of interest was reported by the authors.

Funding

MDP was supported by Prostate UK [S12-008]. VM is supported by the Medical Research Council. This study was supported by U-CAN.GZ is a recipient of the DoD Idea Development Award for New Investigators [PC150263] and a Claudia Adams Barr Award in Innovative Basic Cancer Research.

ORCID

Mieke Van Hemelrijck http://orcid.org/0000-0002-7317-0858

References

[1] Tomlins SA, Rubin MA, Chinnaiyan AM. Integrative biology of prostate cancer progression. Annu Rev Pathol. 2006;1:243–271.

[2] American Cancer Society. Survival rates for prostate cancer. 2016 http://www.cancer.org/cancer/prostate-cancer/detection-diagnosis-staging/survival-rates.html#references.

[3] Dasgupta S, Srinidhi S, Vishwanatha JK. Oncogenic activation in prostate cancer progression and metastasis: molecular insights and future challenges. J Carcinog. 2012;11:4.

[4] Friedl P, Wolf K. Tumour-cell invasion and migration: diversity and escape mechanisms. Nat Rev Cancer. 2003;3(5):362–374.

[5] Lawson CD, Ridley AJ. Rho GTPase signaling complexes in cell migration and invasion. J Cell Biol. 2017.

[6] Baenke F, Peck B, Miess H, et al. Hooked on fat: the role of lipid synthesis in cancer metabolism and tumour development. Dis Model Mech. 2013;6(6):1353–1363.

[7] Flavin R, Peluso S, Nguyen PL, et al. Fatty acid synthase as a potential therapeutic target in cancer. Future Oncol. 2010;6(4):551–562.

[8] Swinnen JV, Roskams T, Joniau S, et al. Overexpression of fatty acid synthase is an early and common event in the development of prostate cancer. Int J Cancer. 2002;98(1):19–22.

[9] Van de Sande T, Roskams T, Lerut E, et al. High-level expression of fatty acid synthase in human prostate cancer tissues is linked to activation and nuclear localization of Akt/PKB. J Pathol. 2005;206(2):214–219.

[10] Wang TF, Wang H, Peng AF, et al. Inhibition of fatty acid synthase suppresses U-2 OS cell invasion and migration via downregulating the activity of HER2/PI3K/AKT signaling pathway in vitro. Biochem Biophys Res Commun. 2013;440(2):229–234.

[11] Li N, Bu X, Tian X, et al. Fatty acid synthase regulates proliferation and migration of colorectal cancer cells via HER2-PI3K/Akt signaling pathway. Nutr Cancer. 2012;64(6):864–870.

[12] Coleman DT, Bigelow R, Cardelli JA. Inhibition of fatty acid synthase by luteolin post-transcriptionally down-regulates c-Met expression independent of proteosomal/lysosomal degradation. Mol Cancer Ther. 2009;8(1):214–224.

[13] Pascual G, Avgustinova A, Mejetta S, et al. Targeting metastasis-initiating cells through the fatty acid receptor CD36. Nature. 2017;541(7635):41–45.

[14] Whale AD, Dart A, Holt M, et al. PAK4 kinase activity and somatic mutation promote carcinoma cell motility and influence inhibitor sensitivity. Oncogene. 2013;32(16):2114–2120.

[15] Dart AE, Box GM, Court W, et al. PAK4 promotes kinase-independent stabilization of RhoU to modulate cell adhesion. J Cell Biol. 2015;211(4):863–879.

[16] King H, Thillai K, Whale A, et al. PAK4 interacts with p85 alpha: implications for pancreatic cancer cell migration. Sci Rep. 2017;7:42575.

[17] Wells CM, Ahmed T, Masters JR, et al. Rho family GTPases are activated during HGF-stimulated prostate cancer-cell scattering. Cell Motil Cytoskeleton. 2005;62(3):180–194.

[18] Bright RK, Vocke CD, Emmert-Buck MR, et al. Generation and genetic characterization of immortal human prostate epithelial cell lines derived from primary cancer specimens. Cancer Res. 1997;57(5):995–1002.

[19] De Piano M, Manuelli V, Zadra G, et al. Lipogenic signalling modulates prostate cancer cell adhesion and migration via modification of Rho GTPases. Oncogene. 2020;39(18):3666–3679.

[20] Hodge RG, Ridley AJ Regulation and functions of RhoU and RhoV. Small GTPases. 2017:1–8.

[21] Czuchra A, Wu X, Meyer H, et al. Cdc42 is not essential for filopodium formation, directed migration, cell polarization, and mitosis in fibroblastoid cells. Mol Biol Cell. 2005;16(10):4473–4484.

[22] Wirth A, Chen-Wacker C, Wu YW, et al. Dual lipidation of the brain-specific Cdc42 isoform regulates its functional properties. Biochem J. 2013;456(3):311–322.

[23] Guan X, Fierke CA. Understanding Protein Palmitoylation: biological Significance and Enzymology. Sci China Chem. 2011;54(12):1888–1897.

[24] Skaar JR, Pagan JK, Pagano M. Mechanisms and function of substrate recruitment by F-box proteins. Nat Rev Mol Cell Biol. 2013;14(6):369–381.

[25] De Piano M, Jones GE, Wells CM. Live cell imaging: tracking cell movement. Standard and Super-Resolution Bioimaging Data Analysis: A Primer. 2017:173–200.

[26] Wells CM, Abo A, Ridley AJ. PAK4 is activated via PI3K in HGF-stimulated epithelial cells. J Cell Sci. 2002;115(Pt 20):3947–3956.